Use of High-Resolution Optical Coherence Tomography in the Surgical Management of Ocular Surface Squamous Neoplasia: A Pilot Study

CAROL L. KARP, CAROLINA MERCADO, NANDINI VENKATESWARAN, MARCO RUGGERI, ANAT GALOR, ARMANDO GARCIA, KAVITHA R. SIVARAMAN, MARIA PAULA FERNANDEZ, ANTONIO BERMUDEZ, AND SANDER R. DUBOVY

• PURPOSE: To evaluate whether high-resolution optical coherence tomography (HR-OCT) can detect histologic tumor margins of ocular surface squamous neoplasia (OSSN).

• METHODS: Eight eyes of 8 patients with OSSN undergoing excision were studied prospectively. Immediately before surgery, the tumor was imaged using commercially available HR-OCT to identify the conjunctival margins of the neoplastic lesion. The tumor borders of the lesion determined by HR-OCT were mapped in relation to an anatomic reference point and transferred intraoperatively. The tumor was excised with 4-mm margins from the visible edge of the lesion with a "no-touch" technique. The specimens were sent for pathologic analysis and the histologic tumor margin was compared to the HR-OCT predicted tumor border.

• RESULTS: Mean age of the 8 patients was 67 ± 9.9 years. Seven were male, 7 were white, and, ethnically, 3 were Hispanic. All 8 tumors were bulbar and in the exposure zone. Seven tumors were limbal. Corneal extension was present in 5. Mean tumor area was 17.5 ± 11.1 mm^2. Clinically, 2 of the tumors were leukoplakic, 1 papillomatous, and 3 gelatinous. A conjunctival tumor margin identified with the HR-OCT coincided with the pathologically confirmed margin mark in all eyes.

• CONCLUSIONS: HR-OCT has the potential to predict histologic tumor margins in OSSN. Optical identification of tumor margins could potentially decrease the incidence of residual positive margins and minimize healthy tissue removal. Advances in HR-OCT technology and integration into a microscope for "real-time" imaging are needed to further improve this technique. NOTE: Publication of this article is sponsored by the American Ophthalmological Society. (Am J Ophthalmol 2019;206:17–31.

Accepted for publication May 28, 2019.

From the Bascom Palmer Eye Institute, University of Miami Miller School of Medicine, Miami, Florida, USA (C.L.K., C.M., N.V., M.R., A.Galor, A.Garcia, K.R.S., M.P.F., A.B., S.R.D.); Miami Veteran Affairs Medical Center, Miami, Florida, USA (A.Galor); and Florida Lions Ocular Pathology Laboratory, Miami, Florida, USA (S.R.D.).

Inquiries to Carol L. Karp, Bascom Palmer Eye Institute, University of Miami Miller School of Medicine, 900 NW 17th St, Miami, FL 33136 USA; e-mail: ckarp@med.miami.edu

OCULAR SURFACE SQUAMOUS NEOPLASIA (OSSN) encompasses a range of neoplastic conditions of the cornea and conjunctiva spanning from dysplasia to carcinoma in-situ to invasive squamous cell carcinoma.[1,2] It is the most commonly occurring nonpigmented ocular surface malignancy.[3–5] Known risk factors include light skin pigmentation, ultraviolet exposure, immunosuppression, human immunodeficiency virus (HIV), smoking, and human papillomavirus (HPV) infection.[6,7] Rarely, OSSN lesions are capable of intraocular and orbital invasion and, less commonly, distant metastasis.[8] Early identification and appropriate management of OSSN tumors is therefore of great importance for optimizing outcomes.

Traditional therapy for OSSN consists of wide local excision, typically with 3- to 4-mm margins, using a no-touch technique.[9,10] The excision is based on the surgeon's clinical impression of the tumor border. Staining of the lesion with rose bengal, lissamine green, and toluidine blue can sometimes help delineate the tumor. Essentially, the surgical excision is based on what the surgeon "sees" plus 3–4 mm of margin removal. Despite the surgeon's best effort, tumor may be present at the excised margin owing to the presence of subclinical disease.

When residual tumor is present at the excised margin, recurrence can reach 56%.[11] Achieving clear margins dramatically reduces the rate of recurrence. Additionally, the use of adjuvant cryotherapy and topical chemotherapeutic agents in addition to wide resection has reduced recurrence after primary excision.[1,10,12,13] Although these adjuvants represent an important advancement in the management of OSSN, the continued practice of taking wide surgical margins can be associated with significant morbidity, including limbal stem cell deficiency and the formation of symblephara.[14]

Ideally, the surgeon would be able to confidently remove the entire tumor at the time of surgical excision, with minimal tissue loss. However, given the limitations of the

0002-9394/$36.00
https://doi.org/10.1016/j.ajo.2019.05.017

standard surgical approach to OSSN management, there is a need for more accurate identification of tumor margins. This would allow removal of the lesion completely and preserve healthy conjunctiva during excision of these tumors. Unfortunately, in terms of surgical evaluation of tumor presence, a gap exists in the identification of tumor margins.

The development of optical coherence tomography (OCT) technology has ushered in a new era of in vivo imaging of the anterior segment of the eye. While originally pioneered for the posterior segment, OCT now provides novel images of anterior segment pathology. This technology has evolved from time-domain devices to spectral-domain and now swept-source devices, providing greater levels of resolution. This has been shown to assist in diagnosis and management of anterior segment diseases.[15] In particular, OCT has been helpful in the management of ocular surface tumors, corneal pathologies, refractive surgery planning, and intraoperative uses, such as in lamellar surgeries.[16–20]

OSSN can be identified by anterior segment OCT machines, specifically the newer devices capable of performing high-resolution OCT (HR-OCT) of 5–7 μm or less.[21,22] Distinctive features of OSSN on HR-OCT allow for its diagnosis and differentiation from other ocular surface pathologies. Subtle findings on these HR-OCT images help to identify the OSSN lesions beyond what is apparent with the clinical examination, providing guidance for clinical management.[21–23]

Studies from our institution and others have shown that HR-OCT is a particularly useful diagnostic tool for identifying ocular surface squamous neoplasia.[22–26] Similar to histopathologic findings of ocular surface squamous neoplasia, HR-OCT images of OSSN show thickened, hyperreflective epithelium and an abrupt transition from abnormal to normal epithelium.[21,22,24,25] These OCT findings have remarkable correlation to the pathologic findings (Figure 1).

Until now, HR-OCT has mainly been described as an in-office tool for diagnosing ocular surface pathology. It has been shown useful in detecting subtle, subclinical OSSN in eyes with complex ocular surface diseases, and following resolution with medical treatment.[22–27] This project takes an innovative, new angle on this technology. This pilot study was devised to determine if we could use this technology as an "optical Mohs" and use the HR-OCT to identify a tumor margin of OSSN. We implemented a commercially available (ENVISU C2200; Bioptigen/Leica Microsystems, Buffalo Grove, Illinois, USA) spectral-domain HR-OCT system to evaluate the utility of HR-OCT in tumor margin mapping prior to surgical resection.

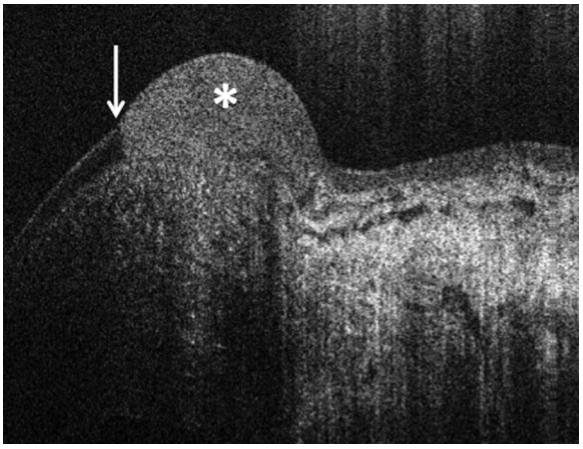

FIGURE 1. High-resolution optical coherence tomography (OCT) of ocular surface squamous neoplasia (OSSN). Classic high-resolution OCT with the Bioptigen device showing classic features of OSSN, including hyperreflective, thickened epithelium (asterisk) with an abrupt transition from normal, thin, dark epithelium to abnormal epithelium (white arrows).

METHODS

THIS PROSPECTIVE STUDY WAS APPROVED BY THE UNIVERSITY of Miami Institutional Review Board and was conducted in accordance with the principles of the Declaration of Helsinki. Written informed consent was obtained from all study participants for both the treatment and participation in the research, and the study was HIPAA compliant.

• **STUDY POPULATION:** Nine eyes of 9 consecutive patients seen at Bascom Palmer Eye Institute and determined to have an ocular surface lesion suspicious for OSSN based on clinical characteristics were included in the study. All patients underwent complete anterior segment examination by a single subspecialist (C.L.K.) in the department of Cornea and External Disease at Bascom Palmer Eye Institute and desired surgical removal of their tumor. Inclusion criteria included an isolated bulbar conjunctival lesion without extension onto palpebral, tarsal, or forniceal conjunctiva. Purely corneal lesions were excluded. Slit-lamp photographs and HR-OCT images of the lesion were obtained of the affected eye of each patient. One patient developed a significant subconjunctival hemorrhage from the retrobulbar block, obscuring all landmarks, and was excluded from the analysis, as intraoperative marking of tumor margins was not possible. Eight remaining patients were thus included and analyzed. Patient records were reviewed for demographic information (age, sex, race, ethnicity) and OSSN risk factors, which included self-reported history of skin cancer or OSSN; HPV; HIV; smoking; presence of pterygium, pinguecula, or prior pterygium surgery; and sun exposure—defined as patient subjectively spending a large quantity of time in the sun.

• **TUMOR CHARACTERISTICS:** Characteristics of the lesion were also documented, including the involved

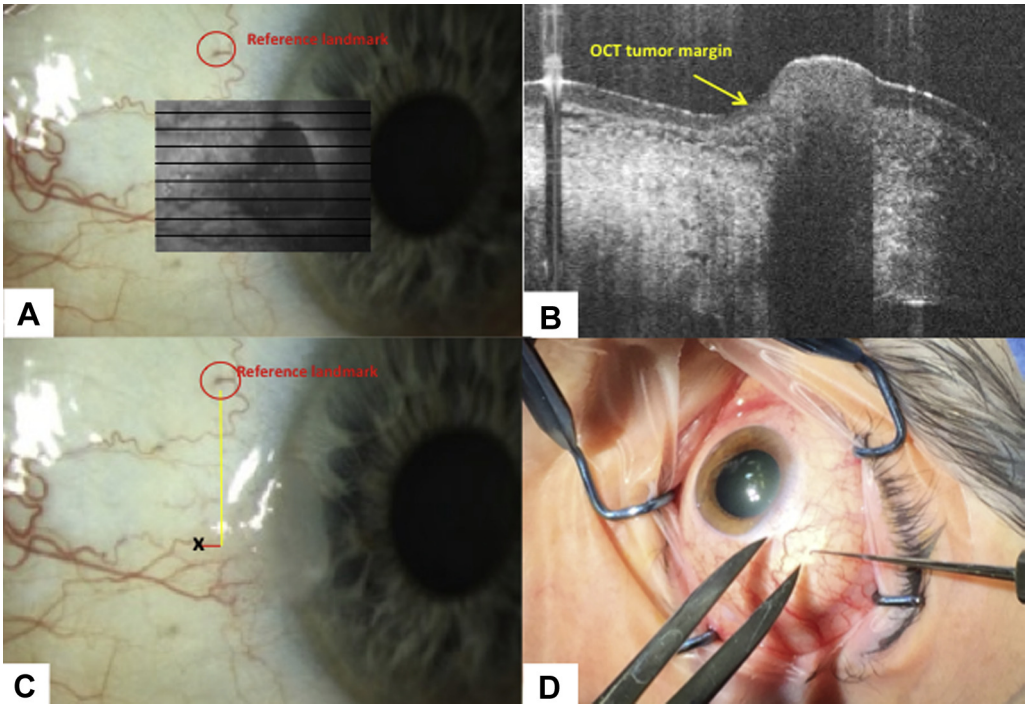

FIGURE 2. Methodology: scanning and transfer of high-resolution optical coherence tomography (HR-OCT) predicted tumor margin points. (A) A reference point was identified of a prominent vessel or marking (red circle). The tumor was scanned to identify lesion margins. The en face overlay is shown in the gray box. (B) Classic OCT findings of epithelial hyperreflectivity and abrupt transition from normal to abnormal were identified (yellow arrow). (C) The internal calipers of the OCT device measured the distance from the reference point to the HR-OCT predicted tumor margin (black x). (D) Example of transfer method of OCT-predicted tumor margin points intraoperatively using calipers and a marked hook.

eye, tumor location, tumor size, and involved ocular structures (conjunctiva, cornea, limbus); unifocality vs multifocality; and appearance (leukoplakic, gelatinous, papillomatous, flat/opalescent). Pathologic grading of the tumor (mild, moderate, or severe carcinoma in situ or invasive squamous cell carcinoma) and margin positivity were also recorded.

• **SPECTRAL-DOMAIN HIGH-RESOLUTION OPTICAL COHERENCE TOMOGRAPHY:** A table-top spectral-domain OCT system (ENVISU C2200; Bioptigen/Leica Microsystems, Buffalo Grove, Illinois, USA) operating at a central wavelength of 840 nm and with 4 μm axial resolution in tissue[28–31] was used for this study. All patients underwent preoperative HR-OCT imaging of the entire suspected OSSN lesion and adjacent tissue. The tumor margin was determined using 3 key characteristics to identify abnormal epithelium affected by OSSN: (1) epithelial thickening; (2) epithelial hyperreflectivity; and (3) an abrupt transition between normal and thickened epithelium. After scanning and reviewing of all images, images that had a defined transition zone were selected.[24]

• **MAPPING OF THE TUMOR MARGINS:** For each eye, the tumor was imaged with slit-lamp photography. One anatomic landmark was identified on the bulbar surface and was used as a fiducial marker (Figure 2A). The selected landmark was typically a prominent branch point in the conjunctival vasculature that was easily identified on the slit-lamp photograph and seen on the en face OCT image. Imaging with the Bioptigen OCT device was used to identify the OSSN tumor margins (Figure 2A,B).

Volume intensity projections of the 3-dimensional OCT data along the depth direction were used to generate gray-scale and en face images of the ocular surface. These images were then registered with the slit-lamp image using the fiducial marker, which was also visible on the OCT en face image.

OCT tumor margin images from the 3-dimensional OCT dataset were analyzed by the subspecialist (C.L.K.). Classic OCT-predicted tumor margins were identified according to the typical OCT features of OSSN as described above. (Figure 2B).

The horizontal and vertical distance between the OCT-identified margin point and the reference landmark on the OCT en face image was then measured using the internal caliper function on the HR-OCT device (yellow and red lines, Figure 2C). The device allowed for real-time simultaneous viewing of both the OCT and the en face image.

Coordinates were placed on a surgical plan and brought to the operating room. In the operating room, the selected points were marked on the eye by finding the reference point and using calipers to measure the predetermined x and y distances from the reference point (Figure 2D).

• **SURGICAL TECHNIQUE:** Intraoperatively, under local anesthesia, the reference landmark was identified. The selected classic tumor margin point identified by HR-OCT was then measured and marked on the ocular surface. For the first 4 patients, this was done after the patient had received a peribulbar block. In 1 case, the block resulted in a subconjunctival hemorrhage obscuring the reference mark and the patient had to be excluded. Following this, all subsequent patients were marked in the operating room under topical anesthesia; then, once marked, the block was given prior to excision.

Initially, the points were marked with a fine marker. On occasion, the ink mark was large and thus later cases were marked with a Sinsky hook (Katalyst Surgical, Chesterfield, Missouri, USA) to allow for smaller and more precise intraoperative markings. The Bioptigen integrated calipers measured distances from the reference mark in the horizontal and vertical meridians to the thousandth of a millimeter. Measurements were rounded and measured as accurately as possible using calipers intraoperatively.

Each lesion was then excised using a standard "no-touch" technique with 4-mm margins from the gross edges of the visible tumor. The margins were marked, and the tissue held by only the peripheral margin being excised. The peripheral margin was cut with scissors and no spreading was done under the tumor. Once the perimeter was cut, the tissue was then reflected off the eye. The field was maintained "dry" with no irrigation to avoid any possible seeding of neoplastic cells. Cryotherapy was applied to the corneal margin when the tumor was limbal, and always to the excised conjunctival edges using a double freeze/slow thaw technique. When cryotherapy was performed on the cornea, the probe was placed straddling the limbus, and the ice ball was allowed to extend and freeze approximately 2 mm onto the cornea. This was also done in a double freeze/slow thaw technique. The conjunctival defect was closed using an amniotic membrane graft secured with fibrin tissue glue.

After excision, each specimen was carefully oriented with respect to its anatomic location and mounted on a piece of cardboard. A simple schematic of the ocular surface was drawn to clarify orientation on the sterile field. These markings were later redrawn in pencil on the cardboard prior to fixation. The OCT-predicted tumor margin, which was measured and marked intraoperatively, was re-marked in the pathology laboratory using permanent ink (Figure 3) prior to fixation. This permanent ink was initially placed with the pointed end of a modified wooden applicator in the early cases and in later cases with a 25 or 30 gauge needle. These techniques were able to mark the OCT-predicted margins but resulted in varying amounts of ink on the mark. The excised nasal, temporal, inferior, superior, and deep tissue margins were marked in the laboratory with permanent ink, as is customary prior to histologic analysis.

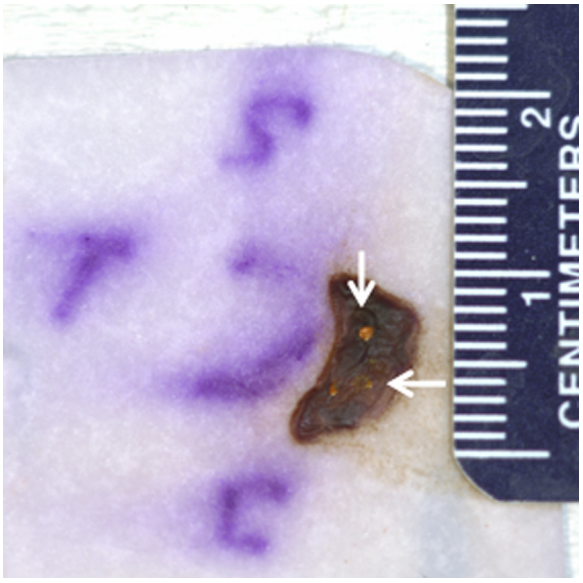

FIGURE 3. Patient 1 conjunctival tumor specimen. Following excision, tumor was placed on paper and oriented in reference to the cornea, superior (S), temporal (T) and inferior (I) locations marked. The transferred high-resolution optical coherence tomography–predicted margins were re-marked with permanent orange dye prior to fixation. Note the variability in the size of the re-marked orange ink dots, with 1 being prominent and the other 2 quite scant (arrows).

Each specimen was carefully oriented with respect to its anatomic location and mounted on a piece of cardboard.

A simple schematic of the ocular surface was drawn to clarify orientation. These markings were later redrawn in pencil on the cardboard prior to fixation. The OCT-predicted tumor margin initially delineated by the intraoperative marking was re-marked using permanent ink (Figure 3). This permanent ink was initially placed with the pointed end of a modified wooden applicator and then was changed to use a 25 or 30 gauge needle. These techniques allowed marking of the OCT-predicted margins but resulted in varying amounts of ink on the mark. The entire specimen on its cardboard platform was then fixed in formalin prior to histologic analysis.

• **HISTOLOGIC ANALYSIS:** All tissue was fixed in formalin and embedded in paraffin. Sections were cut in 5-μm thickness and stained with hematoxylin–eosin. Fifteen to 25 slides were examined per patient. The pathologist (S.R.D.) was asked to evaluate the coincidence of the most prominent OCT-predicted margin ink mark with the actual tumor margin.

TABLE. Demographic and Tumor Characteristics

Patient	Age (Years)	Sex	Laterality	Race	Ethnicity	Involved Quadrant	Clinical Characteristics	Lesion Area (mm^2)	Histopathologic Diagnosis
1	76	F	Right	White	Non-Hispanic	Nasal	Gelatinous	4.5	CIS
2	77	M	Left	White	Non-Hispanic	Nasal	Opalescent	9.7	CIS
3	69	M	Right	White	Hispanic	Nasal	Leukoplakic	2.4	CIS
4	71	M	Right	White	Non-Hispanic	Temporal	Opalescent	23.9	CIS
5	46	M	Right	White	Hispanic	Nasal	Papillomatous	19.3	CIS
6	66	M	Right	Black	Hispanic	Temporal	Gelatinous	20.6	CIS
7	72	M	Left	White	White	Temporal	Gelatinous	33.8	CIN with moderate dysplasia
8	63	M	Right	White	Non-Hispanic	Temporal	Leukoplakic, gelatinous	26.3	CIS

CIN = conjunctival/corneal intraepithelial neoplasia; CIS = conjunctival/corneal intraepithelial neoplasia in situ (full thickness).

• **OUTCOME MEASURES:** The goal of this study was to compare the location of an HR-OCT-guided ink mark to the histologic margin as a proof of principle that HR-OCT can be used to identify OSSN tumor margins. The primary outcome measure was to evaluate the coincidence of the most prominent OCT-predicted histologic ink mark with the actual tumor margin identified pathologically.

RESULTS

• **STUDY POPULATION:** Eight eyes of 8 patients were analyzed. Demographic information is presented in the Table. The mean age of the 8 patients was 67 ± 9.9 years. Seven patients were male, 7 were white, and ethnically, 3 were Hispanic. No patient had a self-reported history of HIV or prior pterygium surgery. One patient had a pinguecula and 1 patient had a self-reported history of HPV. Two patients had a prior history of smoking. All patients reported significant sun exposure, 4 had a history of skin cancer, and 1 had a prior history of OSSN.

• **TUMOR CHARACTERISTICS:** In all cases, the clinical examination revealed clinical characteristics suggestive of OSSN, including leukoplakic, gelatinous, opalescent, or papillomatous lesions. All 8 tumors were bulbar and in the exposure zone. Seven tumors were limbal and corneal extension was present in 5. Clinically, the mean tumor area was 17.5 ± 11.1 mm^2. Two of the tumors appeared leukoplakic, 1 papillomatous, and 3 gelatinous. None of the patients had multifocal lesions or adhesion to the sclera. Three of the lesions were clinically well circumscribed (Patients 3, 5, 8), but most (5 lesions) were subtle with indiscrete margins (Patients 1, 2, 4, 6, 7). The HR-OCT images in all individuals had classic findings of OSSN, including thickened, hyperreflective epithelium and an abrupt transition from normal epithelium to abnormal epithelium. All patients elected surgical excision and agreed to participate in the mapping study.

• **HISTOLOGIC FINDINGS:** All 8 eyes were confirmed to have an OSSN lesion on histopathologic analysis by a board-certified ocular pathologist (S.R.D.). In all cases, the excised lesions showed typical histopathologic characteristics of OSSN, including acanthosis and either partial- or full-thickness faulty maturation. This translated to a diagnosis of conjunctival and corneal intraepithelial neoplasia in all cases. Seven of the 8 cases had full-thickness intraepithelial neoplasia in situ and 1 case had moderate dysplasia. There were no positive conjunctival margins from the wide excisions, and none were invasive squamous cell carcinoma.

The pathologist was asked to evaluate the most prominently inked HR-OCT predicted margin mark in each case. All of the 8 studied eyes had OCT-predicted tumor margins coinciding with the actual tumor margins seen on histopathologic sections (Figures 4–9). Some of the cases had a large amount of ink at the marked junction, and some had very scant ink with this technique. Case scenarios of analyzed patients are described below.

Case 1. A 76-year-old white woman with a history of skin cancer and sun exposure presented with a 1-year history of a corneal and conjunctival tumor in the right eye nasally (Figure 4A). The area on the cornea was gelatinous, and the adjacent conjunctival component was subtle. It was not easy to see any distinct conjunctival tumor margins. In-office imaging with HR-OCT revealed classic findings of hyperreflective thickened epithelium with an abrupt transition from normal to abnormal.

Preoperatively, OCT images were acquired at the nasal conjunctival limbal area of the right eye from approximately the 2 o'clock to the 5 o'clock position. Tumor margins were identified by the OCT (Figure 4B). A reference landmark was selected of a blood vessel with an obvious notch (Figure 4C). The reference landmark was chosen for ease of identification in the operating room as well as for en face measurements. The distance from the reference mark to the tumor margin was

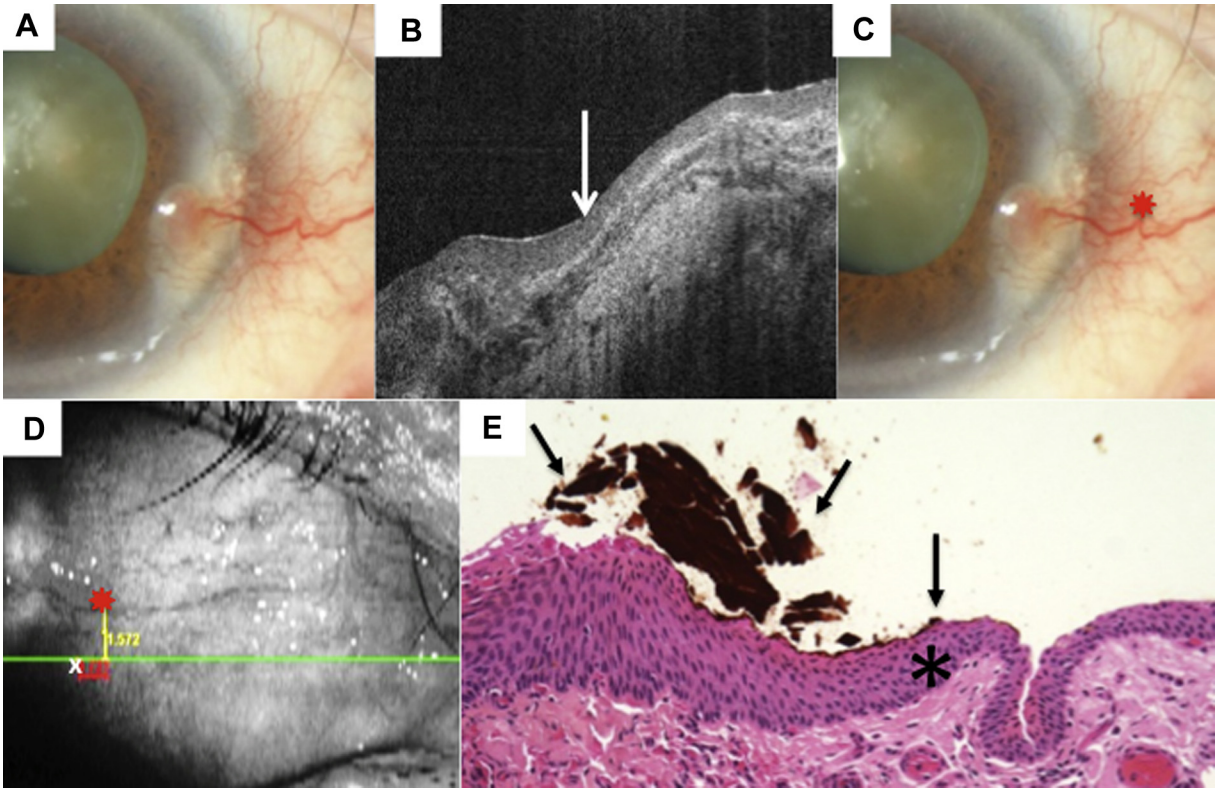

FIGURE 4. Patient 1 corneal and conjunctival tumor. (A) Slit-lamp photograph of corneal and limbal ocular surface squamous neoplasia (OSSN) lesion, right eye from Patient 1. (B) High-resolution optical coherence tomography (HR-OCT) cut with predicted tumor margin denoted by white arrow. (C) Slit-lamp photograph of corneal and limbal OSSN lesion with reference landmark (red star). (D) OCT en face reconstruction of ocular surface with reference landmark denoted by red star and measurement to HR-OCT-predicted tumor margin (white x) done by internal calipers from reference landmark vertically and horizontally. (E) Examination of the excised conjunctiva discloses faulty epithelial maturational sequencing that extends up to full thickness (carcinoma in situ), with the area of tumor margin (asterisk) adjacent to the transition of unremarkable and dysplastic epithelium. The OCT-predicted mark (orange pigment, black arrows) coincides with the pathologically identified margin (hematoxylin-eosin; original magnification ×200).

performed using internal calipers on the OCT device and rounded to one tenth of a millimeter. As seen in Figure 4D, vertical and horizontal distances were documented from the reference point to the OCT-predicted tumor margin. Three margin points were then transferred to the surgical worksheet. The OCT-predicted margins were marked in the operating room using a fine marker on the patient's bulbar conjunctiva. Four-millimeter margins were then taken in the "no-touch" technique and cryotherapy.

Once removed from the patient, the tissue was oriented on the filter paper with superior, nasal, temporal, and corneal margins indicated (Figure 3). Once passed off the field, the orientation of superior, inferior, and temporal was re-marked in pencil for the pathologist, as the surgical pen ink on the paper often dissolves. Similarly, the OCT-identified tumor margins were re-marked with permanent ink in the pathology laboratory with permanent orange ink. This was done with the pointed wood end of a cotton-tip applicator. As seen in Figure 3, the dot sizes were variable, with some large and some scant.

The most prominently inked OCT-predicted margin was then compared to the actual histopathologic tumor margin. On histopathology, the OCT-predicted tumor margin mark coincided with the histologic margin junction (Figure 4E). As noted in Figure 3, an excess of approximately 2–3 mm existed between the OCT-predicted margin and the empiric 4-mm margin for the clinically observed margin.

Case 2. A 77-year-old white man who was an avid boater, scuba diver, and former smoker presented with a subtle gelatinous corneal and conjunctival tumor in the left eye nasally. The conjunctival margins of this lesion were not easily visualized (Figure 5A).

OCT images were performed at the limbal area nasally in the left eye. In contrast to the difficulty evaluating the tumor margins by clinical examination, the

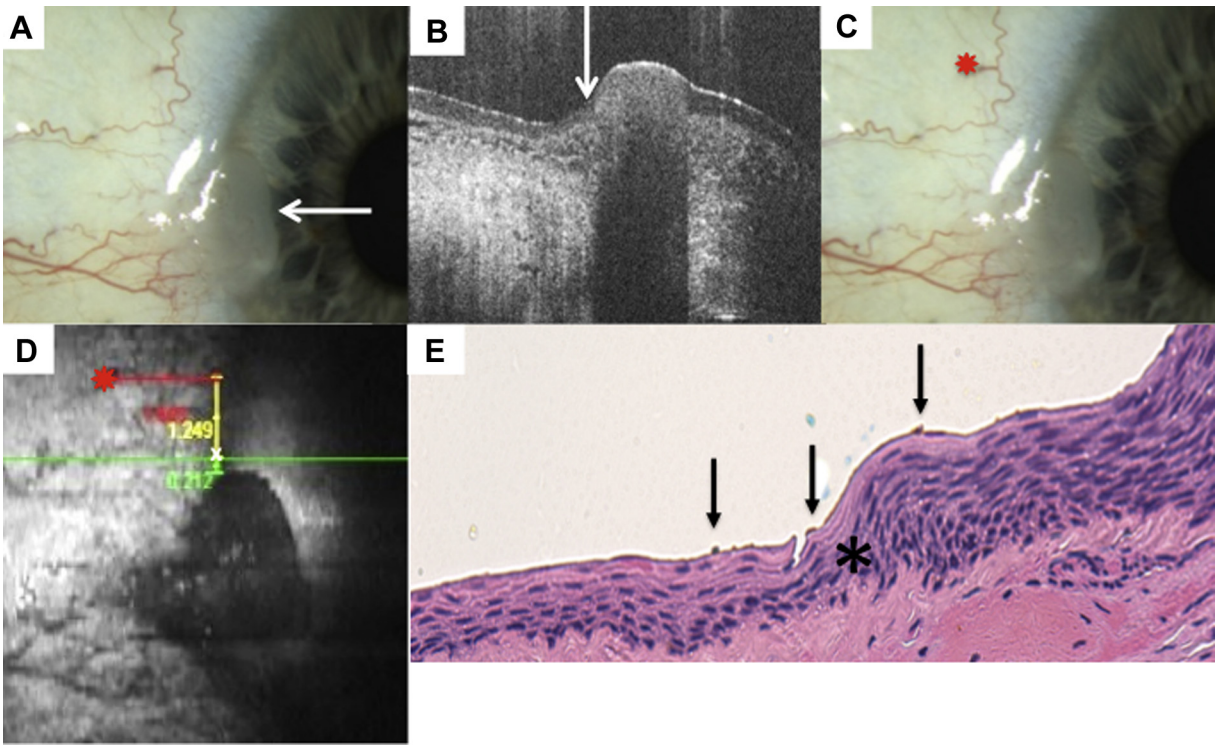

FIGURE 5. Patient 2 corneal and conjunctival tumor. (A) Slit-lamp photograph of left eye from Patient 2 showing subtle elevated gelatinous lesion on the cornea (arrow) and conjunctiva consistent with limbal ocular surface squamous neoplasia. (B) High-resolution optical coherence tomography (HR-OCT) cut with predicted tumor margin denoted by white arrow. (C) Slit-lamp photograph of left eye showing selected reference landmark (red star). (D) OCT en face reconstruction of ocular surface with reference landmark denoted by red star and measurement to superior HR-OCT predicted tumor margin (white x) from reference landmark with internal calipers. (E) Examination of the excised conjunctiva discloses faulty epithelial maturational sequencing that extends up to full thickness (carcinoma in situ). The tumor margin (asterisk) is located at the transition of unremarkable and dysplastic epithelium. The OCT-predicted mark (subtle orange pigment, black arrows) coincides with pathologically identified margin (hematoxylin-eosin; original magnification ×200).

tumor margins were well visualized by the HR-OCT (Figure 5B). A reference landmark of a right-angle branching blood vessel was identified (Figure 5C). Tumor margins were visualized by the HR-OCT (Figure 5B). Three points were then transferred to the surgical plan. The distance from the reference mark to the tumor margin was performed using internal calipers, as seen in Figure 5D. The vertical and horizontal distances were documented from the reference point to the OCT-predicted tumor margin. The OCT-predicted margins were marked in the operating room using a fine marker on the patient's bulbar conjunctiva. In this case, the conjunctival tumor margins were not well seen, and the OCT-predicted margin did not reflect a clinically visible tumor edge. Four-millimeter margins were then taken with a "no-touch" technique based on the OCT marks and the surgeon's best estimation of the indistinct margin location. Cryotherapy was applied in double freeze/slow thaw manner to the limbus and conjunctival borders.

After removal and orientation, this time a 30 gauge needle was used to re-mark the tissue at the OCT-indicated locations with permanent ink. The needle was used in an attempt to have a smaller marked area of ink compared to Patient 1. With this method, the ink mark was smaller compared to the technique used in the first patient (using the wooden end of a cotton-tip applicator). Even with the pathologist evaluating the most prominent mark, that ink was subtle, but visible, coinciding with the pathologic tumor margin (Figure 5E).

Case 3. A 69-year-old white Hispanic man presented with a discrete 2 mm × 3 mm leukoplakic lesion nasally on the right eye at the limbus (Figure 6A). He reported years of sun exposure.

OCT images were performed at the limbal area nasally. Thickening and hyperreflectivity were seen on OCT (Figure 6B). A reference landmark was identified as a looped conjunctival vessel. As above, the distance from the reference mark to the tumor margin was measured

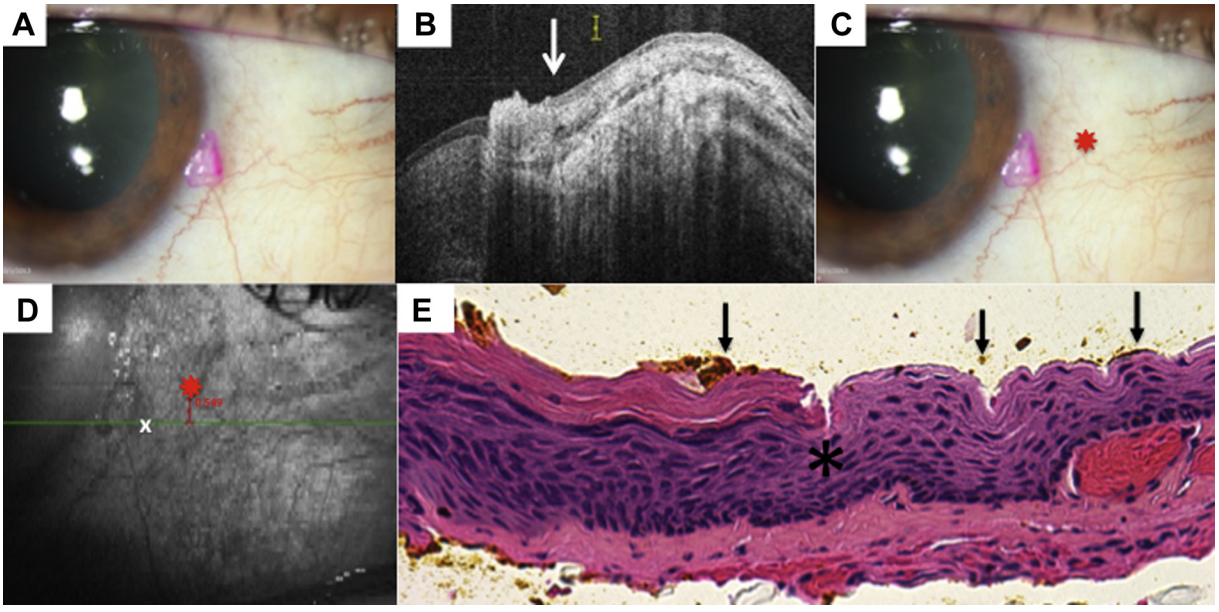

FIGURE 6. Patient 3 conjunctival tumor with leukoplakia. (A) Slit-lamp photograph of right eye from Patient 3 with a discrete, leukoplakic lesion consistent with ocular surface squamous neoplasia. (B) High-resolution optical coherence tomography (HR-OCT) cut with predicted tumor margin denoted by white arrow. Note thickening and strong hyperreflectivity over tumor. Adjacent bulbar conjunctiva has normal thickness but remains somewhat hyperreflective epithelium adjacent to tumor, likely secondary to actinic changes. (C) Slit-lamp photograph of right eye showing selected reference landmark (red star). (D) OCT en face reconstruction of ocular surface with reference landmark denoted by red star and measurement to HR-OCT predicted tumor margin (white x) with internal calipers. (E) Examination of the excised conjunctiva discloses faulty epithelial maturational sequencing that extends up to full thickness with overlying hyperkeratosis (carcinoma in situ); the area of tumor margin (asterisk) is present adjacent to the transition of variably acanthotic and dysplastic epithelium. The OCT-predicted tumor margin mark (orange pigment, black arrows) coinciding with pathologically identified margin (hematoxylin-eosin; original magnification ×400).

with internal calipers for vertical and horizontal measurement from the reference point (Figure 6C,D). This was then rounded and transferred to the surgical plan and marked in the operating room using a fine marker on the patient's bulbar conjunctiva. Two points were transferred, and 4-mm margins were then taken in the "no-touch" technique with cryotherapy. After removal and orientation on the marked paper, a 30 gauge needle was used to mark the tissue at the OCT-indicated locations with permanent ink. In this case, an attempt was made to release more ink than what was done in Case 2. In 1 of the marked points, scant ink was released. In the other, adequate ink was placed. The evaluated HR-OCT-predicted margin coincided with the pathologic tumor margin, and the ink marking was a good quantity (Figure 6E).

Case 4. A 71-year-old white man presented with a pinguecula temporally on the right eye. It had been present for many years. He had a history of sun exposure, skin cancer, and smoking. Clinically the lesion appeared slightly atypical, and OCT imaging revealed that the gelatinous subtle lesion was indeed OSSN.

HR-OCT images performed at the bulbar and limbal area temporally revealed distinct thickening with an abrupt junction. A reference landmark was identified of a blood vessel loop. Three points were transferred to the surgical plan. Instead of a marking pen, the OCT-predicted margins were marked in the operating room using a marked Sinsky hook on the patient's bulbar conjunctiva. This was in the hope of having less ink spreading. Four-millimeter margins were then taken with cryotherapy. After removal and orientation on the marked paper, a 30 gauge needle was again used to mark the tissue at the OCT-indicated locations with permanent ink. Similar to Case 2, (Figure 5, Case 2), the surgical ink was on the OCT-identified mark, but was very subtle. Even the most prominent mark was scant but showed the OCT-predicted margin coinciding with the pathologic tumor margin.

Case 5. A 46-year-old white Hispanic man with a history of cutaneous melanoma presented with a 3-month history of an elevated, well-circumscribed papillomatous conjunctival tumor in the right eye nasally (Figure 7A). The HR-OCT revealed classic findings for OSSN (Figure 7B).

A reference landmark was identified (Figure 7C) that was an easily visible Y branching of a blood vessel.

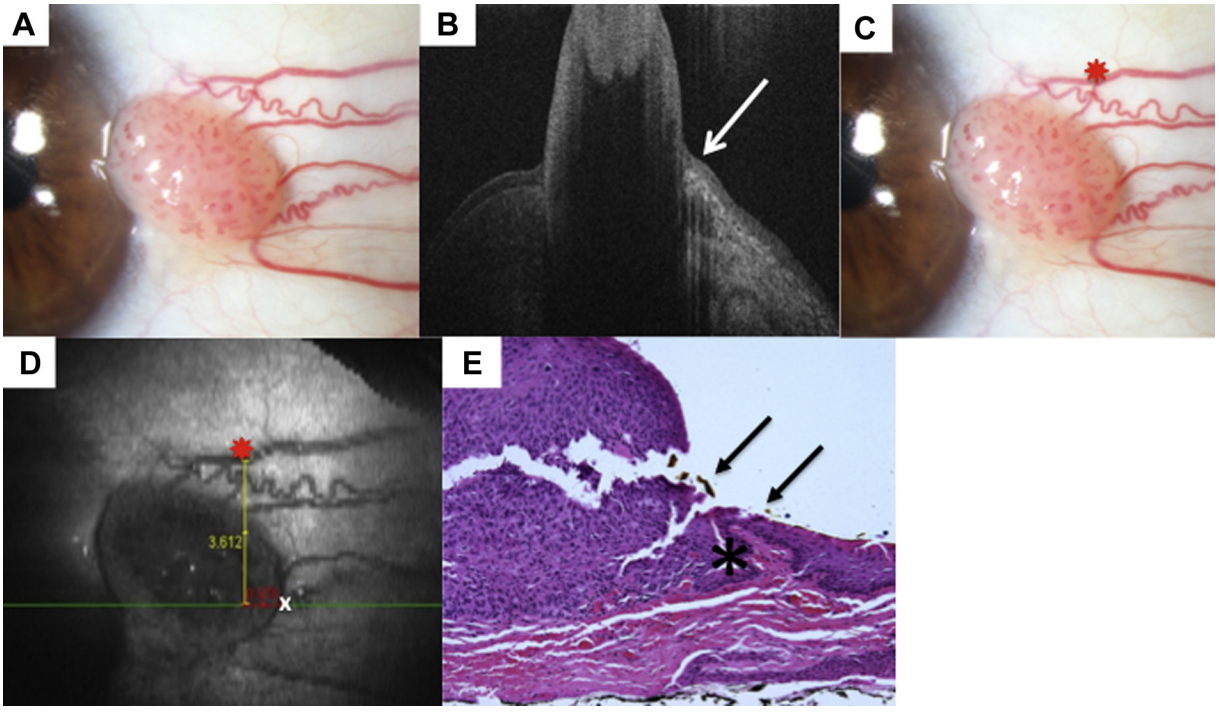

FIGURE 7. Patient 5 papillomatous conjunctival tumor. (A) Slit-lamp photograph of a papillary ocular surface squamous neoplasia from Patient 5. (B) High-resolution optical coherence tomography (HR-OCT) image of tumor margin denoted by white arrow. (C) Slit-lamp photograph reference landmark (red star), a Y bifurcation of a conjunctival vessel. (D) OCT en face reconstruction of ocular surface with reference landmark denoted by red star. Internal calipers used to measure the distance from the predicted tumor margin (white x) to the reference landmark. (F) Examination of the excised conjunctiva discloses faulty epithelial maturational sequencing that extends up to full thickness in a variable papillary configuration (carcinoma in situ, papillary) with the area of OCT predicted tumor margin (orange pigment, arrows) adjacent to the transition of unremarkable and thickened, dysplastic epithelium (asterisk) (hematoxylin-eosin; original magnification ×200).

HR-OCT images were performed nasally over the lesion. The distance from the reference mark to the tumor margin was performed using internal calipers for vertical and horizontal measurement from the reference point. The points were then approximated and transferred to the surgical plan. The HR-OCT-predicted margin was marked in the operating room using a marked Sinsky hook on the patient's bulbar conjunctiva. Excision was performed with 4-mm margins, as above. In this well-circumscribed papillomatous lesion, the OCT-predicted mark was right at the edge of the elevated tumor (Figure 7D).

After removal and orientation on the marked paper, a 30 gauge needle was again used to mark the tissue at the OCT-indicated location with permanent ink. The OCT-predicted margins coincided with histologic margins, as seen in Figure 7E. The ink marking in this case was minimal but easily visible at the tumor border.

Case 6. A 66-year-old black Hispanic man with a history of longstanding sun exposure presented with a diffuse lesion temporally on the right eye (Figure 8A). It had both conjunctival and corneal components. Some conjunctival melanosis was also evident in the lesion. In-office imaging with HR-OCT revealed classic findings for OSSN (Figure 8B). The conjunctival edges of the temporal lesion were difficult to discern clinically.

A reference landmark was identified as a looped vessel (Figure 8C). The distance from the reference mark to the tumor margin was performed using internal calipers (Figure 8D). The OCT-predicted margin was marked in the operating room using a marked Sinsky hook on the patient's bulbar conjunctiva. This tumor did not have obvious conjunctival tumor borders and the OCT mark was approximately 1 mm outside of the visible gelatinous lesion. Four-millimeter margins were then taken in the "no-touch" technique. After removal and orientation on the marked paper, a 25 gauge needle was used to mark the tissue at the HR-OCT-indicated locations with permanent ink. Since the prior 3 patients had very little permanent ink on the pathology slides, this time it was intended to release more permanent ink with the needle. The OCT-predicted margins correlated well with the pathologic tumor margin and more ink was noted than in the prior cases (Figure 8E).

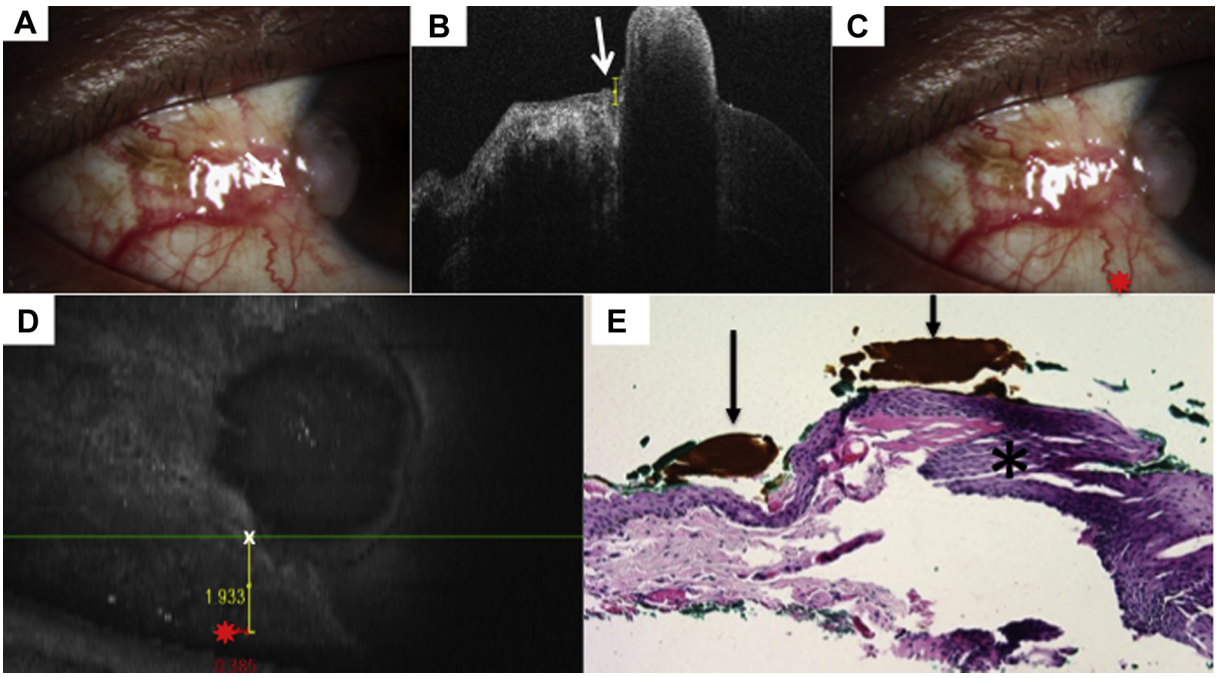

FIGURE 8. Patient 6 corneal and conjunctival tumor. (A) Slit-lamp photograph of diffuse conjunctival ocular surface squamous neoplasia with opalescent corneal component. Note conjunctival melanosis in this patient with dark complexion. (B) High-resolution optical coherence tomography (HR-OCT) cut with predicted tumor margin denoted by arrow. (C) Slit-lamp photograph of right eye showing selected reference landmark (red star) of looped vessel. (D) OCT en face reconstruction of ocular surface with reference landmark denoted by red star and measurement of inferior HR-OCT-predicted tumor margin (white x) from reference landmark. (E) Examination of the excised, tangentially sectioned conjunctiva discloses faulty epithelial maturational sequencing that extends up to full thickness (carcinoma in situ) with the area of OCT predicted tumor margin (arrows; orange pigment) adjacent to the transition of unremarkable and dysplastic epithelium (asterisk) (hematoxylin-eosin; original magnification ×200).

Case 7. Case 7 involved a 72-year-old white man with a history of multiple skin cancers who presented with a nonlimbal bulbar conjunctival lesion temporally in the left eye. It had been diagnosed as episcleritis for many months. The lesion was mobile with indistinct clinical margins. HR-OCT was highly suggestive of OSSN.

A reference landmark was identified and OCT images were performed of the bulbar temporal lesion. The distance from the reference mark to the tumor margin was performed using internal calipers. Again the OCT-predicted margin was marked in the operating room using a marked Sinsky hook on the patient's bulbar conjunctiva. Four-millimeter margins were then taken. After removal and orientation on the marked paper, a 30 gauge needle was used to mark the tissue at the OCT-indicated locations with permanent ink in an attempt to have a smaller marked area than that from Case 6. This time, similar to Cases 2 and 4 (Figure 5, Case 2), the ink was again very scant. However, the pathologist was able to identify ink of the OCT-predicted margin coinciding with the pathologic tumor margin.

Case 8. The last case involved a 63-year-old white man with a self-reported history of long sun exposure as well as HPV from venereal condyloma acuminata who presented with a highly elevated temporal conjunctival lesion in the right eye. The lesion stained with rose bengal and had classic features of OSSN by OCT (Figure 9A). The white elevated lesion was obvious neoplasia, but it was not clear the extent of neoplasia in the surrounding, somewhat gelatinous ring, which did not stain with the rose bengal.

OCT images were performed and identified tumor margins (Figure 9B). Interestingly, this OCT showed tumor extending beyond the obvious tumor "ball." A kinked blood vessel was used as a fiducial mark (Figure 9C). As seen in the en face image, this predicted OCT margin was quite distal (approximately 2 mm) from the obvious tumor (Figure 9D). Two points were transferred. This was done using a marked hook in the operating room.

Four-millimeter margins were then taken with cryotherapy. After removal, a 30 gauge needle was used to mark the tissue at the HR-OCT-indicated locations with permanent ink. One mark was scant and the other was prominent. At this prominent mark, the histopathology revealed a classic abrupt transition from normal to abnormal epithelium (Figure 9E). The OCT-predicted margin concurred nicely with the pathologic tumor margin. The ink quantity was ideal.

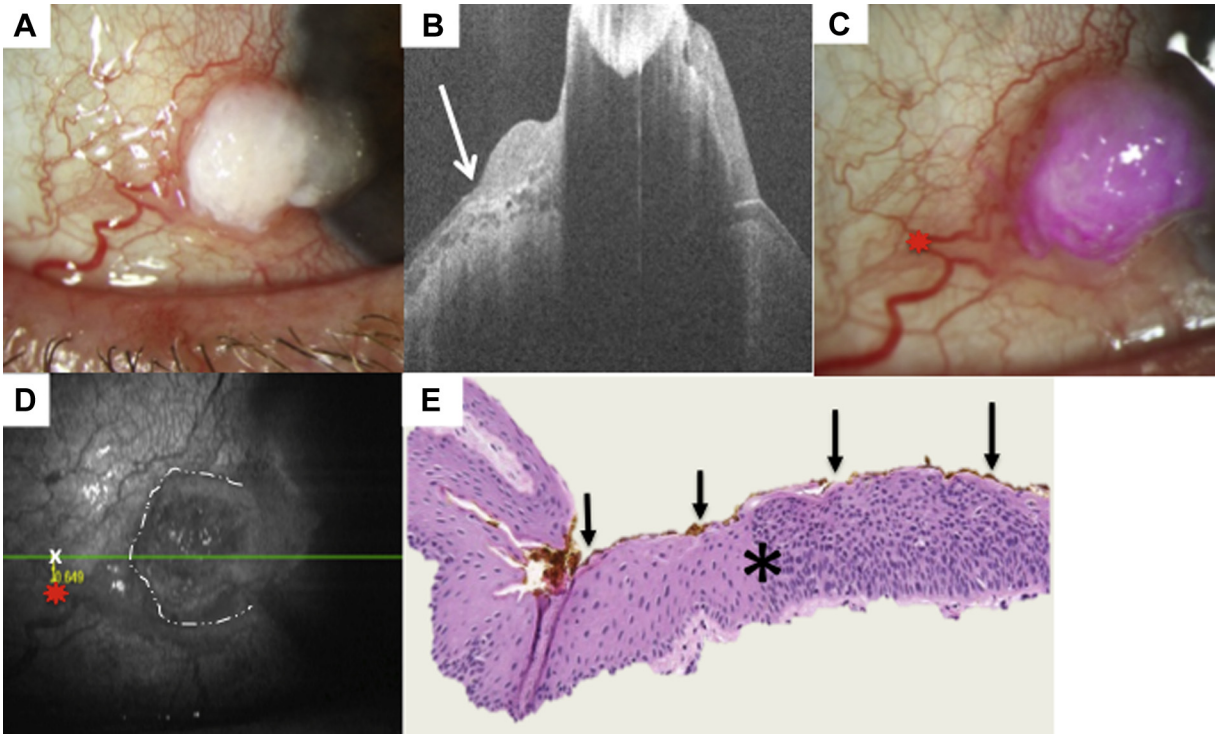

FIGURE 9. Patient 8 elevated conjunctival tumor. (A) Slit-lamp photograph of limbal ocular surface squamous neoplasia lesion from Patient 8. (B) High-resolution optical coherence tomography (HR-OCT) image indicates tumor margin denoted by white arrow. (C) Slit-lamp photograph of limbal OSSN lesion with reference landmark (red star). (D) OCT en face reconstruction of ocular surface with reference landmark denoted by red star and measurement of temporal tumor margin. Of note, the HR-OCT-predicted tumor margin (white x) was temporal to the obvious discrete tumor seen (dashed white lines). (E) Examination of the excised conjunctiva discloses faulty epithelial maturational sequencing that extends up to full thickness (carcinoma in situ) with the area of OCT predicted tumor margin (arrows, orange pigment) coinciding with the transition of unremarkable and dysplastic epithelium (asterisk) (hematoxylin-eosin; original magnification ×200).

DISCUSSION

THE PURPOSE OF THIS PILOT STUDY WAS TO DEMONSTRATE proof of concept that HR-OCT could successfully identify tumor margins as confirmed by histopathology. We were able to identify 1 OCT-predicted point in each case coinciding with the histopathologic tumor borders. To our knowledge, this is the first study to evaluate the HR-OCT in this manner.

Medical vs surgical treatment of OSSN continues to be a topic of debate. Although monotherapy with topical chemotherapeutic agents has increasing popularity for the treatment for OSSN,[32–36] many practitioners still report that they perform surgical excision as part of their standard management, regardless of tumor size.[37]

When performing surgical excision, the "no-touch technique" is commonly implemented, which involves removal of a large (3–4 mm) margin past the visible edge of the tumor.[9] The principle behind wide margin excision is that microscopic tumor may extend past its grossly visible margin. Therefore, additional healthy tissue must be sacrificed in order to increase the likelihood that diseased tissue is excised in its entirety. Achieving negative margins is of utmost importance, as over half of OSSN tumors with positive surgical margins may recur.[11]

In the skin, a Moh's-style excision with pathologic margin control is commonly employed with great success.[38] This, along with frozen section margin control, has been tried for conjunctival tumors.[39] Frozen section control for conjunctival tumors has had limited utilization. Most pathologists consider frozen section evaluation of mucosal tumors to be inaccurate in assessing intraepithelial dysplasia. The primary purpose of this pilot study was to show a proof of concept that the optical evaluation of the ocular surface with HR-OCT could successfully identify tumor margins.

The advent of OCT now affords the ability to perform an "optical biopsy" of ocular tissues.[40] This technology is able to provide cross-sectional, detailed, in vivo images of ocular tissues. Although initially used for imaging the posterior pole, it is now able to provide excellent resolution for the anterior segment and ocular surface. As OCT technology has evolved with the advent of spectral-domain OCT devices, resolution of 5 μm is possible (high resolution) and even lower, of less than 5 μm (ultra-high resolution). Unlike ultrasound, which has resolution of about 50 μm,

the use of light gives higher resolution than ever before. This is owing to the short wavelength of infrared light and the wide bandwidth of the light sources used in OCT machines. Resolution of 7 μm or less allows visualization of the structural details in the corneal epithelium, corneal stroma, and conjunctiva.[16–18,20–27]

Historically, OCT was first used for ocular structures in the early 1990s.[41,42] These time-domain OCT machines were the first generation of OCT technology. With time-domain OCT, images were produced as the reference mirror crossed linearly over the eye. Based on the reflectivity and depth of each tissue, the device produced individual A-scans, which were then combined to create a cross-sectional image (B-scan).[42–44] These early-generation time-domain OCT devices provided resolutions of about 10–20 μm.[43] Time-domain OCT devices were hindered by slow image acquisition time owing to the need for the reference mirror to physically move across the imaging field. This provided fewer A-scans per second (100–200) and thus was especially susceptible to artifact and distortion from patient motion. One advantage of the devices was that the longer wavelength of 1300–1310 nm allowed for excellent depth of penetrance and allowed for good visibility of the anterior segment, including iris and lens. Time-domain OCT machines were later improved to allow for over 2000 A-scans/second, but resolution remained in the 15–25 μm range.[43,45,46]

The next advance in OCT technology for the anterior segment was the development of spectral-domain OCT. These devices no longer used the mobile reference mirror described above. Instead, a spectrometer and high-speed camera are used to simultaneously capture the reflections generated from structures located at different depths in the tissue.[45] This spectral information is then transformed using a mathematical tool developed by French mathematician Joseph Fourier to obtain a reflectivity profile of the sample, which is the produced OCT image. This more efficient detection system is often called "Fourier-domain" and allows for scan speeds increased to over 70 000 A-scans/second.[47] These devices were originally used to image structures in the posterior pole, and adaptive lenses were required for anterior segment imaging. These devices provided improved resolution of 4–7 μm and allowed for detailed imaging of the corneal stroma and epithelium.[43,47–49]

The current resolution of HR-OCT devices allows for the identification of OSSN and its differentiation from other ocular surface lesions and has excellent morphologic correlation with histopathology.[15,18,21,22,24,25] Our group first studied the use of ultra-HR-OCT for ocular surface diseases and specifically OSSN using a custom-built device of 2–3 μm of axial resolution. We were able to demonstrate excellent correlation between the OCT images and the corresponding histopathology. We identified key characteristics of OSSN on HR-OCT, which, as mentioned above, include a thickened hyperreflective epithelium with an abrupt transition from normal to abnormal.[24] Using our custom device, we were able to determine with a receiver operating curve that a thickness of approximately 140 μm had a sensitivity of 94% and a specificity of 100% for OSSN.[24] We then studied its use for OSSN with a commercially available high-resolution device of 5–7 μm, which revealed similarly excellent results. With the commercially available HR-OCT and using a thickness cutoff of 120 μm, the sensitivity and specificity for OSSN was 100%.[26]

As this technology has been found to have excellent diagnostic specificity and sensitivity in the outpatient setting for diagnosis of OSSN,[24,26] we performed this pilot study to determine whether this technology could be used to identify tumor margins intraoperatively. As demonstrated by Figures 4–9, 1 HR-OCT-predicted tumor margin for each case was evaluated and coincided with actual histologic tumor margins. Three of the 8 cases had a well-circumscribed lesion, and 5 of the cases were more subtle or diffuse. Instinctively we would suspect that this technology would be most useful in the more subtle or diffuse lesions. Indeed, this technique was very helpful in cases where the tumor border was not easily visualized. Interestingly, in Case 8, which was well delineated, the OCT found the tumor margin to be peripheral to the obvious area of the tumor and rose bengal staining (Figure 9).

This concept of an "optical Moh's" is exciting and intriguing. We found that we could indeed identify tumor borders using HR-OCT and translate this to create a surgical map to successfully identify tumor margins intraoperatively. The ability to outline and identify the microscopic extent of OSSN tumors has significant implications for the surgical management of this disease. With a more accurate idea of the true tumor margins, surgeons can potentially reduce the incidence of leaving residual disease. In addition, potentially less surrounding tissue will be sacrificed and thus reduce the risk of ocular surface complications such as scarring, limbal stem cell deficiency, and ocular motility restriction.[12,14]

With all studies, there are limitations. While the HR-OCT has excellent specificity and sensitivity to diagnose OSSN, multiple scans are sometimes required to identify the exact tumor margin.[24,26] Most tumor margins show the classic characteristics of thickening, hyperreflectivity, and an abrupt transition from abnormal to normal epithelium. However, in some cases the non-neoplastic epithelium is thin, but may be somewhat hyperreflective due to actinic changes in the tissue. In such cases, the border is characterized by the thickened hyperreflective epithelium transitioning to thin, normal-thickness epithelium but not the dark-to-white, abrupt change. Furthermore, current OCT technology is able to show morphologic and internal reflectivity changes in the epithelium but is not yet able to show cellular changes such as atypia.

We were able to identify the tumor margins by OCT and confirm them by pathology, in all 8 bulbar conjunctival tumors. However, we found that the technique of marking and ink transfer was not ideal. We learned that marking of

the eye prior to excision is best done with topical anesthesia. In 1 case, a subconjunctival hemorrhage from the retrobulbar block precluded visualization of the reference mark and the patient was excluded from the study. After that occurrence, we marked the patients under topical anesthesia in the operating room and then blocked the patient, which rendered the process more time-consuming. In addition, since this technology is not yet available as a "real-time" integrated intraoperative system with the microscope, we needed to use an anatomic landmark on the conjunctiva as a reference point. The marking of the OCT-predicted tumor margins on the ocular surface was initially performed with a sterile marking pen but was subsequently changed to using a Sinsky hook in attempts to make smaller, more precise markings. Furthermore, markings were approximated intraoperatively from the internal caliper measurements from the HR-OCT device, another step that could be obviated with a real-time device. Once transferred to filter paper and brought to the pathology laboratory, the specimens were re-marked with permanent ink prior to formalin fixation to confirm our OCT-predicted margins. It was challenging to place the "right" amount of ink, as some cases had more ink than desired and some, only scant ink.

Despite these challenges, we were able to confirm the most prominent OCT-predicted tumor margin mark coinciding with the histopathologic tumor border in all 8 cases. Ideally, we would have been able to evaluate all the marks, but this was not always possible owing to scant ink. These challenges demonstrate the need for an integrated HR-OCT within the operating room microscope, which would have bypassed many of these more cumbersome steps and provided an en face overlay for the excision. Intraoperative OCT imaging integrated into the operating microscope[50] has been useful for anterior chamber surgeries such as endothelial transplantation, but the ophthalmic microscope–integrated OCT devices commercially available at this time do not have the resolution needed to accurately detect the margins of these epithelial tumors. Microscope-integrated OCT systems also currently have a fixed scanning direction, which prevents proper alignment of the OCT scanning beam to target the location of all ocular surface tumors. Hand-held OCT systems do exist, but they are limited by motion artifact and still require the marking step. With an integrated HR-OCT intraoperative system, a full mapping and orientation of the tumor margin could be performed in real time, without the need for point transfer and ink marking. Once such a system is available, a future study could compare the physicians' clinical impression of tumor margins with the OCT-predicted and actual tumor margins. Finally, the clinical outcomes of OCT-guided excisions can then be compared to traditional surgery.

In conclusion, this pilot study showed that a commercially available HR-OCT can successfully predict tumor margins that coincide with histopathologic tumor borders. The horizon of OCT guided surgical excisions is indeed promising and exciting. These results will hopefully encourage the development of high-resolution "real-time" intraoperative OCT devices for use in ocular surface tumor excisions.

FINANCIAL SUPPORT: NIH CENTER CORE GRANT P30EY014801, RPB UNRESTRICTED AWARD AND CAREER DEVELOPMENT Awards, Department of Veterans Affairs, Veterans Health Administration, Office of Research and Development, Clinical Sciences Research EPID-006-15S (Dr. Galor), R01EY026174 (Dr.Galor), The Dr. Ronald and Alicia Lepke Grant, The Lee and Claire Hager Grant, The H. Scott Huizenga Grant, The Grant and Diana Stanton-Thornbrough, The Robert Baer Family Grant, The Emilyn Page and Mark Feldberg Grant, The Jose Ferreira de Melo Grant, Richard and Kathy Lesser Grant, The Michele and Ted Kaplan Grant and the Richard Azar Family Grant (institutional grants). Financial Disclosures: The following authors have no financial disclosures: Carol L. Karp, Carolina Mercado, Nandini Venkateswaran, Marco Ruggeri, Anat Galor, Armando Garcia, Kavitha R. Sivaraman, Maria Paula Fernandez, Antonio Bermudez, and Sander R. Dubovy. All authors attest that they meet the current ICMJE criteria for authorship.

Other Acknowledgments: Drs Madura Joag and Brian Alder (Bascom Palmer Eye Institute, University of Miami Miller School of Medicine, Miami, Florida, USA) participated in data acquisition.

REFERENCES

1. Galor A, Karp CL, Oellers P, et al. Predictors of ocular surface squamous neoplasia recurrence after excisional surgery. *Ophthalmology* 2012;119(10):1974–1981.
2. Kiire CA, Srinivasan S, Karp CL. Ocular surface squamous neoplasia. *Int Ophthalmol Clin* 2010;50(3):35–46.
3. Shields CL, Demirci H, Karatza E, Shields JA. Clinical survey of 1643 melanocytic and nonmelanocytic conjunctival tumors. *Ophthalmology* 2004;111(9):1747–1754.
4. Lee GA, Hirst LW. Incidence of ocular surface epithelial dysplasia in metropolitan Brisbane: a 10-year survey. *Arch Ophthalmol* 1992;110(4):525–527.
5. Sun EC, Fears TR, Goedert JJ. Epidemiology of squamous cell conjunctival cancer. *Cancer Epidemiol Biomarkers Prev* 1997;6(2):73–77.
6. Kiire CA, Dhillon B. The aetiology and associations of conjunctival intraepithelial neoplasia. *Br J Ophthalmol* 2006;90(1):109–113.
7. Carreira H, Coutinho F, Carrilho C, Lunet N. HIV and HPV infections and ocular surface squamous neoplasia: systematic review and meta-analysis. *Br J Cancer* 2013;109(7):1981–1988.
8. Yousef YA, Finger PT. Squamous carcinoma and dysplasia of the conjunctiva and cornea: an analysis of 101 cases. *Ophthalmology* 2012;119(2):233–240.

9. Shields JA, Shields CL, dePotter P. Surgical management of conjunctival tumors: The 1994 B. McMahan Lecture. *Arch Ophthalmol* 1997;115(6):808–815.
10. Nanji AA, Moon CS, Galor A, Sein J, Oellers P, Karp CL. Surgical versus medical treatment of ocular surface squamous neoplasia: a comparison of recurrences and complications. *Ophthalmology* 2014;121(5):994–1000.
11. Tabin G, Levin S, Snibson G, Loughnan M, Taylor H. Late recurrences and the necessity for long-term follow-up in corneal and conjunctival intraepithelial neoplasia. *Ophthalmology* 1997;104(3):485–492.
12. Peksayar G, Altan-Yaycioglu R, Onal S. Excision and cryosurgery in the treatment of conjunctival malignant epithelial tumours. *Eye (Lond)* 2003;17(2):228–232.
13. Siganos C, Kozobolis V, Christodoulakis E. The intraoperative use of mitomycin-C in excision of ocular surface neoplasia with or without limbal autograft transplantation. *Cornea* 2002;21(1):12–16.
14. Palamar M, Kaya E, Egrilmez S, Akalin T, Yagci A. Amniotic membrane transplantation in surgical management of ocular surface squamous neoplasias: long-term results. *Eye (Lond)* 2014;28(9):1131–1135.
15. Wang J, Abou Shousha M, Perez VL, et al. Ultra-high resolution optical coherence tomography for imaging the anterior segment of the eye. *Ophthalmic Surg Lasers Imaging* 2011;42 Suppl:S15–S27.
16. Venkateswaran N, Galor A, Wang J, Karp CL. Optical coherence tomography for ocular surface and corneal diseases: a review. *Eye Vis (Lond)* 2018;5:13.
17. Han SB, Liu YC, Noriega KM, Mehta JS. Applications of anterior segment optical coherence tomography in cornea and ocular surface diseases. *J Ophthalmol* 2016;2016:4971572.
18. Vajzovic LM, Karp CL, Haft P, et al. Ultra high-resolution anterior segment optical coherence tomography in the evaluation of anterior corneal dystrophies and degenerations. *Ophthalmology* 2011;118(7):1291–1296.
19. Shousha MA, Yoo SH, Kymionis GD, et al. Long-term results of femtosecond laser-assisted sutureless anterior lamellar keratoplasty. *Ophthalmology* 2011;118(2):315–323.
20. Iovieno A, Sharma DP, Wilkins MR. OCT visualization of corneal structural changes in traumatic dislocation of LASIK flap. *Int Ophthalmol* 2012;32(5):459–460.
21. Shousha MA, Karp CL, Perez VL, et al. Diagnosis and management of conjunctival and corneal intraepithelial neoplasia using ultra high-resolution optical coherence tomography. *Ophthalmology* 2011;118(8):1531–1537.
22. Atallah M, Joag M, Galor A, et al. Role of high resolution optical coherence tomography in diagnosing ocular surface squamous neoplasia with coexisting ocular surface diseases. *Ocul Surf* 2017;15(4):688–695.
23. Ong SS, Vora GK, Gupta PK. Anterior segment imaging in ocular surface squamous neoplasia. *J Ophthalmol* 2016;2016:5435092.
24. Kieval JZ, Karp CL, Abou Shousha M, et al. Ultra-high resolution optical coherence tomography for differentiation of ocular surface squamous neoplasia and pterygia. *Ophthalmology* 2012;119(3):481–486.
25. Thomas BJ, Galor A, Nanji AA, et al. Ultra high-resolution anterior segment optical coherence tomography in the diagnosis and management of ocular surface squamous neoplasia. *Ocul Surf* 2014;12(1):46–58.
26. Nanji AA, Sayyad FE, Galor A, Dubovy S, Karp CL. High-resolution optical coherence tomography as an adjunctive tool in the diagnosis of corneal and conjunctival pathology. *Ocul Surf* 2015;13(3):226–235.
27. Singh S, Mittal R, Ghosh A, Tripathy D, Rath S. High-resolution anterior segment optical coherence tomography in intraepithelial versus invasive ocular surface squamous neoplasia. *Cornea* 2018;37(10):1292–1298.
28. Shroff R, Francis M, Pahuja N, Veeboy L, Shetty R, Sinha Roy A. Quantitative evaluation of microdistortions in Bowman's layer and corneal deformation after small incision lenticule extraction. *Transl Vis Sci Technol* 2016;5(5):12.
29. Pahuja N, Shroff R, Pahanpate P, et al. Application of high resolution OCT to evaluate irregularity of Bowman's layer in asymmetric keratoconus. *J Biophotonics* 2017;10(5):701–707.
30. Kumar M, Shetty R, Jayadev C, Dutta D. Comparability and repeatability of pachymetry in keratoconus using four noncontact techniques. *Indian J Ophthalmol* 2015;63(9):722–727.
31. Shetty R, Nagaraja H, Pahuja NK, Jayaram T, Vohra V, Jayadev C. Safety and efficacy of epi-bowman keratectomy in photorefractive keratectomy and corneal collagen cross-linking: a pilot study. *Curr Eye Res* 2016;41(5):623–629.
32. Parrozzani R, Lazzarini D, Alemany-Rubio E, Urban F, Midena E. Topical 1% 5-fluorouracil in ocular surface squamous neoplasia: a long-term safety study. *Br J Ophthalmol* 2011;95(3):355–359.
33. Hirst LW. Randomized controlled trial of topical mitomycin C for ocular surface squamous neoplasia: early resolution. *Ophthalmology* 2007;114(5):976–982.
34. Nanji AA, Sayyad FE, Karp CL. Topical chemotherapy for ocular surface squamous neoplasia. *Curr Opin Ophthalmol* 2013;24(4):336–342.
35. Vann RR, Karp CL. Perilesional and topical interferon alfa-2b for conjunctival and corneal neoplasia. *Ophthalmology* 1999;106(1):91–97.
36. Russell HC, Chadha V, Lockington D, Kemp EG. Topical mitomycin C chemotherapy in the management of ocular surface neoplasia: a 10-year review of treatment outcomes and complications. *Br J Ophthalmol* 2010;94(10):1316–1321.
37. Adler E, Turner J, Stone D. Ocular surface squamous neoplasia: a survey in the changes of standard of care from 2003 to 2012. *Cornea* 2012;32(12):1558–1561.
38. Patel TN, Patel SB, Franca K, Chacon AH, Nouri K. Mohs micrographic surgery: history, technique, and advancements. *Skinmed* 2014;12(5):289–292.
39. Buus DR, Tse DT, Folberg R, Buuns DR. Microscopically controlled excision of conjunctival squamous cell carcinoma. *Am J Ophthalmol* 1994;117(1):97–102.
40. Karp CL. Evolving technologies for lid and ocular surface neoplasias: is optical biopsy a reality? *JAMA Ophthalmol* 2017;135(8):852–853.
41. Izatt JA, Hee MR, Swanson EA, et al. Micrometer-scale resolution imaging of the anterior eye in vivo with optical coherence tomography. *Curr Opin Ophthalmol* 1994;112(12):1584–1589.
42. Huang D, Swanson EA, Lin CP, et al. Optical coherence tomography. *Science* 1991;254(5035):1178–1181.
43. Ramos JL, Li Y, Huang D. Clinical and research applications of anterior segment optical coherence tomography - a review. *Clin Exp Ophthalmol* 2009;37(1):81–89.

44. Simpson T, Fonn D. Optical coherence tomography of the anterior segment. *Ocul Surf* 2008;6(3):117–127.
45. Jancevski M, Foster CS. Anterior segment optical coherence tomography. *Semin Ophthalmol* 2010;25(5-6):317–323.
46. Radhakrishnan S, Rollins AM, Roth JE, et al. Real-time optical coherence tomography of the anterior segment at 1310 nm. *Arch Ophthalmol* 2001;119(8):1179–1185.
47. Kiernan DF, Mieler WF, Hariprasad SM. Spectral-domain optical coherence tomography: a comparison of modern high-resolution retinal imaging systems. *Am J Ophthalmol* 2010;149(1):18–31.
48. Maeda N. Optical coherence tomography for corneal diseases. *Eye Contact Lens* 2010;36(5):254–259.
49. Leite MT, Rao HL, Zangwill LM, Weinreb RN, Medeiros FA. Comparison of the diagnostic accuracies of the Spectralis, Cirrus, and RTVue optical coherence tomography devices in glaucoma. *Ophthalmology* 2011;118(7):1334–1339.
50. Das S, Kummelil MK, Kharbanda V, et al. Microscope integrated intraoperative spectral domain optical coherence tomography for cataract surgery: uses and applications. *Curr Eye Res* 2015;1–10.